Pattern Recognition for Biomedical Imaging and Image-Guided Diagnosis

Nikita V. Orlov, John Delaney, D. Mark Eckley, Lior Shamir, and Ilya G. Goldberg
Laboratory of Genetics
National Institute of Aging/NIH
251 Bayview Blvd, Baltimore, MD
{ norlov, delaneyjd, dme, shamirli, igg }@nih.gov

Abstract— **Pattern recognition techniques can potentially be used to quantitatively analyze a wide variety of biomedical images. A challenge in applying this methodology is that biomedical imaging uses many imaging modalities and subjects. Pattern recognition relies on numerical image descriptors (features) to describe image content. Thus, the application of pattern recognition to biomedical imaging requires the development of a wide variety of image features. In this study we compared the efficacy of different techniques for constructing large feature spaces. A two-stage method was employed where several types of derived images were used as inputs for a bank of feature extraction algorithms. Image pyramids, subband filters, and image transforms were used in the first-stage. The feature bank consisted of polynomial coefficients, textures, histograms and statistics as previously described [1]. The basis for comparing the performance of these feature sets was the biological imaging benchmark described in [2]. Our results show that a set of image transforms (Fourier, Wavelet, Chebyshev) performed significantly better than a set of image filters (image pyramids, sub-band filters, and spectral decompositions). The transform technique was used to analyze images of H&E-stained tissue biopsies from two cancers: lymphoma (three types of malignancies) and melanoma (benign, primary, and five secondary tumor sites). The overall classification accuracy for these cancer data sets was 97%.**

I. INTRODUCTION

The objective of this study was the comparative analysis of different approaches to identify reliable ways of automatic image classification in a broad range of image types in biological and biomedical domains. Medical diagnosis relies on the identification of morphological features by expert surgical pathologists. The use of imaging as an assay in the biological sciences relies on either manual interpretation, or algorithms developed specifically for the image type and subject. Automated, robust, and quantitative image analysis methods are in great demand in these two disciplines.

Pattern recognition relies on training by example rather than manually constructed visual models, which implies that this technique can be used to analyze a much larger variety of image types compared to purpose-built algorithms. To be broadly applicable, image classification relies on a wide variety of image content descriptors. Image transforms and filters combined with a standardized bank of feature extraction algorithms can have a multiplicative effect on the quantity and variety of image features presented to a classification algorithm. In this study, we compare the effectiveness of features derived from several image transforms to those derived from several filters in classifying a benchmark set of biological images as well as two sets of images related to cancer diagnosis from H&E-stained biopsies.

II. TWO-STAGE SCHEME FOR CONSTRUCTING FEATURE SPACE

In this two-stage scheme, we used filters and transforms to generate different derived images that were then used as inputs for a standardized bank of feature extraction algorithms (see Fig. 1).

A. Image Filters for Multi-Layer Decompositions

The first step is applying Image filters. We define an Image filter ϕ as a simple remapping of the original image onto modified pixel plane $\mathbf{F}$: $\phi(\mathbf{I}) = \mathbf{F}$, or a series of such pixel planes:

$$\mathbf{F}_{(\alpha)} : \phi(\mathbf{I}) = \bigcup\nolimits_{\alpha} \mathbf{F}_{(\alpha)} . \quad (1)$$

Filters like in (1) produce either multi-scale, or multi-band, or spectral decompositions of the original pixel plane. The set of transforms used were those defined in previous work $\mathbf{I} \xrightarrow{\text{FB}} \vec{\psi}(\mathbf{I})$, [1] describing the WND-CHARM algorithm, and included Fourier, Wavelet, and Chebyshev. We used three ways to construct derived images (see in Fig. 2): Image Pyramids (IP) [3], Subband Filters (SF) [4] and image Transforms (WND) [1].

B. Feature Banks for Pixel Planes

Image features are quantitative representations of image content [5]. Feature Bank (FB) is a set of algorithms for

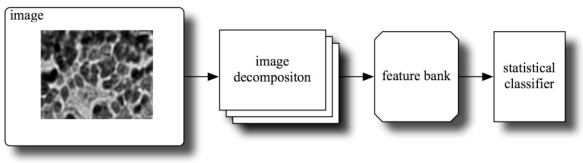

Fig. 1. Constructing feature spaces includes stages of image decomposition with Image filters (or Transforms) and feature extraction on each layer of decomposed pixel planes.

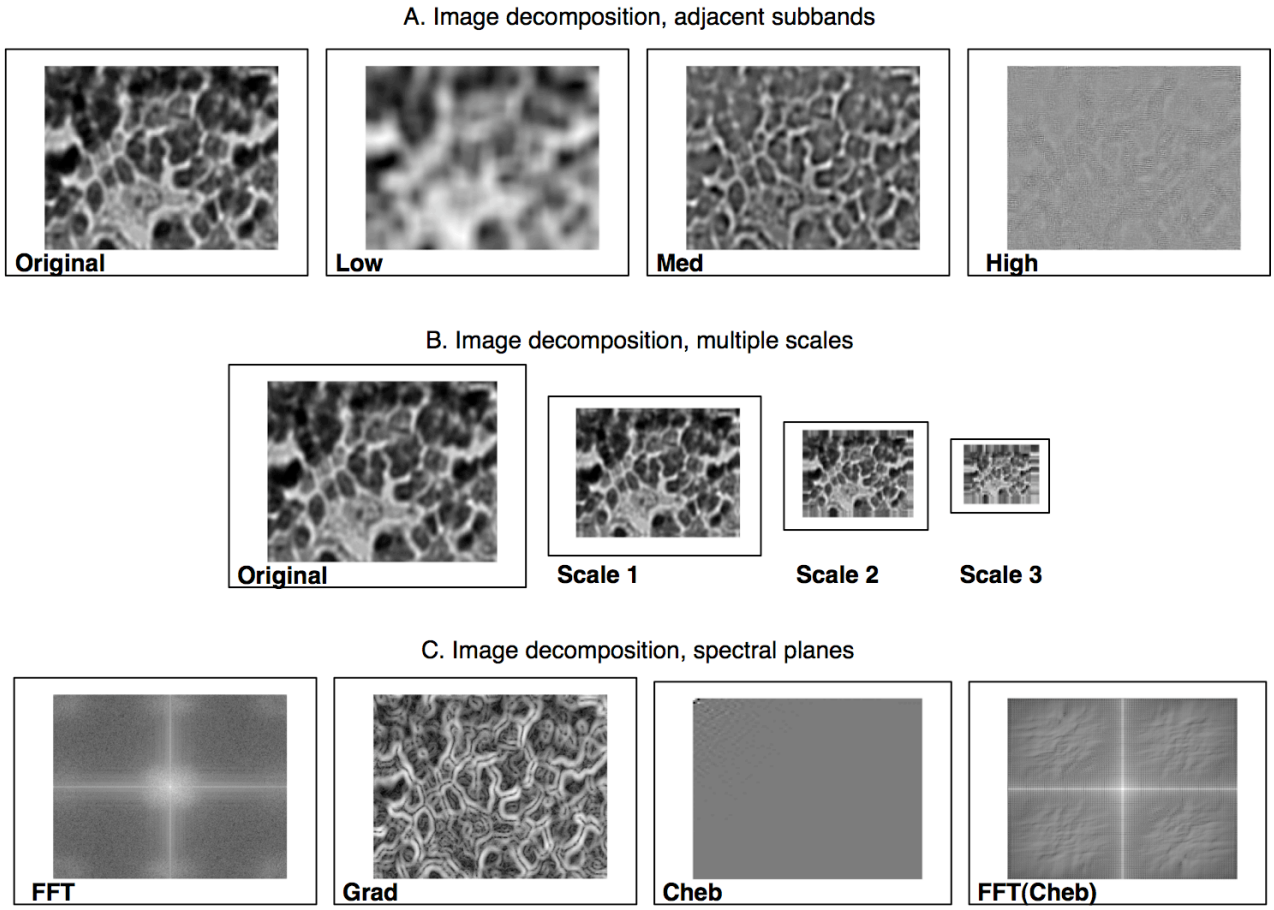

Fig. 2. Examples of Image decompositions with frequency subband filters (A), Image pyramid (B), and image Transforms (C). Patterns shown in decomposition layers are distinct.

computing image features on a given pixel plane. FB could be thought of as a conversion of the original $M \times N$ pixel plane to a $L \times 1$ feature vector:

$$\mathbf{I} \xrightarrow{\text{FB}} \vec{\psi}\left(\mathbf{I}\right), \tag{2}$$

In our work we use low level features that are *global* (not specific to the concrete image application). The full description of out set calculating (2) could be found in [1]. The set includes descriptors based on polynomial coefficients (we used Chebyshev, Chebyshev-Fourier, and Zernike polynomials), textures (Haralick, Gabor, and Tamura families were computed), and several multi-purpose families, including Radon, singular values, multi-scale histograms, moments calculated from a four-directional comb filter, edge and blob statistics.

C. Chains Based on Image Filters and Transforms

The next step in the approach is in applying FBs (2) to all pixel planes $\left\{\mathbf{F}_{(\alpha)}\right\}$ resulting from filters (1). This results in series of feature vectors $\bigcup_{\alpha} \vec{\psi}\left(\mathbf{F}_{(\alpha)}\right)$, specific to the parent filter ϕ. We call those feature vectors the computational chains. The resulting multi-scale (or multi-spectral) feature set promises to become more efficient, as a result of combining several layers of image content. The transform-based chain that we used included Fourier transform, Chebyshev and wavelet (level one details only) transforms. Additionally, it had two *compound* transforms: Wavelet of Fourier and Chebyshev of Fourier.

D. Feature Weights

As features based on (1) are not application-specific, not all of them are equally useful. We employed a ranking scheme based on Fisher score [6], rewarding features with high separation between different classes and uniform within the same class. Our classifier is based on a neighbor distance algorithm with distances measured in this weighted feature space [1].

III. EXPERIMENTS ON BIOLOGICAL IMAGE SETS

We present a numerical comparison of several different chains based on three types of derived images. In our comparisons we employed several biological image collections [2]. The pollen image set contained seven types of pollen. Two other sets contain sub-cellular compartments from Chinese Hamster Ovary (CHO), and HeLa cell lines [7]. Two other sets were images of the worm *C. elegans*, including body wall muscle stained with phalloidin and the pharynx terminal bulb imaged with differential interference contrast (DIC) [8]. Our comparisons showed that the chain

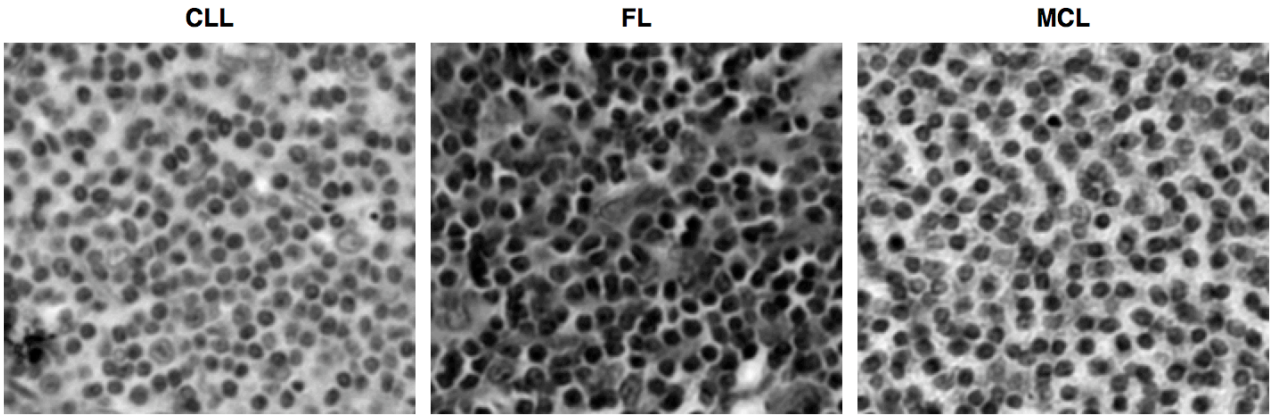

Fig. 3. Examples three types of malignancies in the lymphoma image set. Here 20x objective was employed (1/30th of the image size is shown).

using transforms was consistently more accurate than chains based on sub-band or image pyramid filters (Table I).

IV. CLASSIFYING MALIGNANT TISSUES

We used the image transform chain to classify images from two datasets related to cancer diagnosis from H&E-stained tissue biopsies. The first set is a representative collection of lymph node biopsies from three types of malignancies: chronic lymphatic leukemia, follicular lymphoma and mantle cell lymphoma. Imaging was done in bright-field using a 20x objective and an RGB camera. Rrepresentative images of the three lymphoma classes are shown in Fig. 3. We employed no preprocessing of data, segmentation, ROI selection, or contrast enhancement. The highest classification rate achieved on this set was 0.97.

The second dataset consisted of benign, primary and five secondary melanoma tumors. The data in this set were images of stained tissue micro-arrays (TMA) printed on glass slides. The data contained seven malignant tissue types. We reserved test sets setting aside a portion of randomly selected images, using remaining spots for training. The average classification accuracy obtained on all random splits (and all seven classes) was 0.93.

TABLE I
COMPARISON OF SF, IP AND TR CHAINS. SHOWN: CLASSIFICATION SCORE, PER CENT; ERROR IN BRACKETS

Set	SF	IP	WND
Pollen	85(2)	89(1)	96(2)
CHO	94(2)	94(3)	95(1)
HeLa	79(3)	82(2)	86(1)
C.elegans, BWM	60(2)	60(2)	57(2)
C.elegans, TB	41(2)	53(1)	55(2)
Average	**71.8**	**75.6**	**77.8**
Lymphoma	-	-	97(1)
Melanoma TMA	-	-	93(3)

V. CONCLUSIONS

The approach of translating image content into multi-level feature space with use of image transforms demonstrated its high efficacy in recognizing real-world malignancies in two different cancer sets.

ACKNOWLEDGMENT

This research was supported by the Intramural Research Program of the NIH, National Institute of Aging. The authors gratefully acknowledge reviewers' comments.

REFERENCES

[1] N. Orlov, L. Shamir, T. Macura, J. Johnston, D. M. Eckley, and I. G. Goldberg, "WND-CHARM: Multi-purpose image classification using compound image transforms," *Pattern Recognition Letters,* vol. 29, pp. 1684-1693, 2008.

[2] L. Shamir, N. Orlov, D. M. Eckley, T. J. Macura, and I. G. Goldberg, "IICBU 2008: a proposed benchmark suite for biological image analysis," *Medical & Biological Engineering & Computing,* vol. 46, pp. 943-947, July 31, 2008 2008.

[3] E. H. Adelson, C. H. Anderson, J. R. Bergen, P. J. Burt, and J. M. Ogden, "Pyramid methods in image processing," *RCA Engineer,* vol. 29, pp. 33-41, Nov/Dec 1984.

[4] P. Burt and E. Adelson, "The Laplacian pyramid as a compact image code," *IEEE Transactions on Communications,* vol. 31, pp. 532-540, 1983.

[5] A. Rosenfeld, "From image analysis to computer vision: an annotated bibliography, 1955-1979," *Computer Vision and Image Understanding,* vol. 84, pp. 298-324, 2001.

[6] K. Fukunada, *Introduction to statistical pattern recognition*. San Diego: Academic Press, 1990.

[7] R. F. Murphy, "Automated interpretation of protein subcellular location patterns: implications for early detection and assessment," *Annals of the New York Academy of Sciences,* vol. 1020, pp. 124-131, 2004.

[8] N. Orlov, J. Johnston, T. Macura, C. Wolkow, and I. Goldberg, "Pattern recognition approaches to compute image similarities: application to age related morphological change," in *International Symposium on Biomedical Imaging: From Nano to Macro*, Arlington, VA, 2006, pp. 1152-1156.